OPTOELECTRONICS (2)

Lecture 2.5
Photodetectors

Mohammad Ali Mansouri- Birjandi

Department of Electrical and Computer Engineering
University of Sistan and Baluchestan (USB)
mansouri@ece.usb.ac.ir
mamansouri@yahoo.com

مرجع

Emmanuel Rosencher, and Borge Vinter,

"Optoelectronics",

English edition Cambridge University Press,

2004

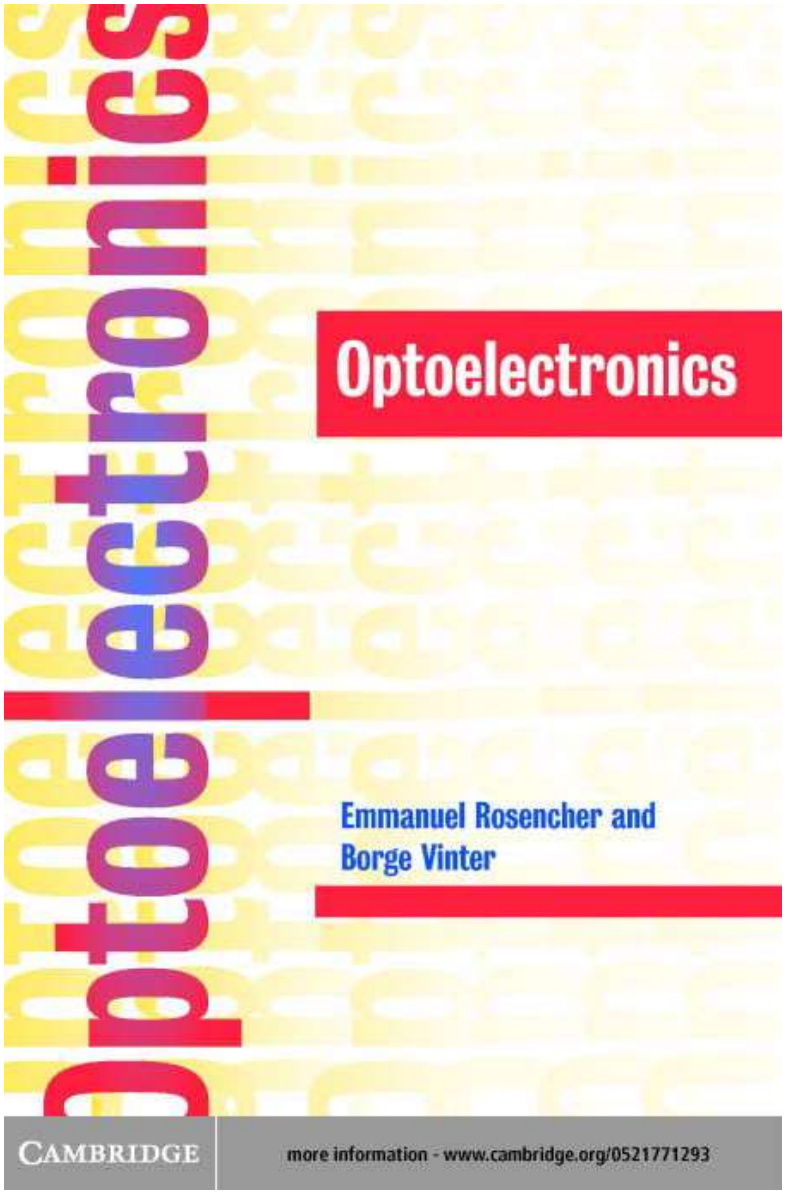

فهرست مطالب

1

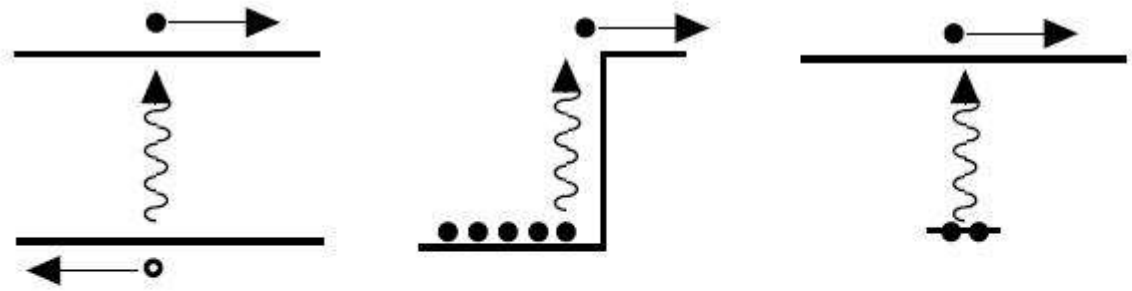

Fig. 11.1. Three types of quantum detection based on: (*a*) band to band transitions which generate electron–hole pairs, (*b*) internal photoemission above a potential barrier, and (*c*) transition from a bound state to a continuum.

2

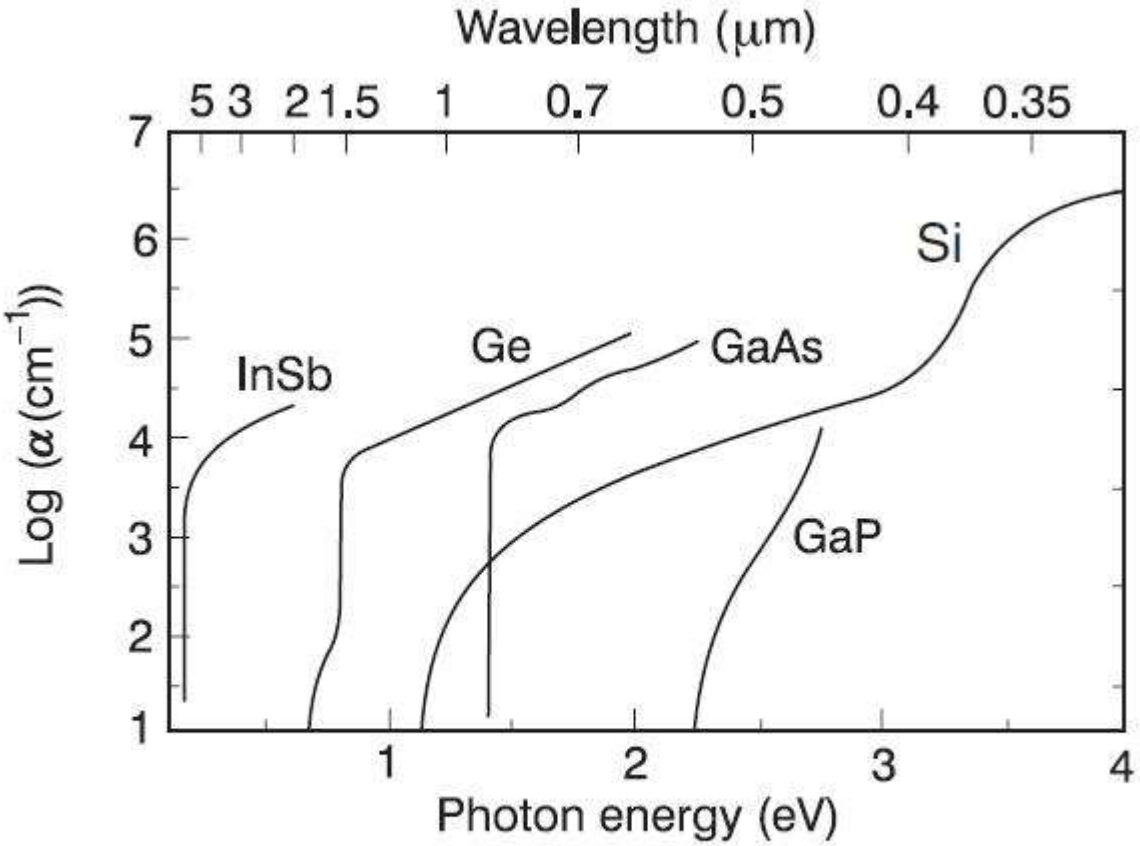

Fig. 11.2. Spectral dependence of absorption for a few important semiconductors

3

Table 11.1. *Values for the recombination lifetimes* τ, *mobilities* μ_n *and* μ_p, *300 K bandgaps, and dielectric constants for important semiconductors*

Material	τ (s)	μ_n ($cm^2\,V^{-1}\,s^{-1}$)	μ_p ($cm^2\,V^{-1}\,s^{-1}$)	E_g (eV)	ε_r
Si	10^{-4}	1350	480	1.12	11.8
Ge	10^{-2}	3900	1900	0.67	16
GaAs	10^{-6}	8500	400	1.42	13.2
InAs	10^{-7}	33 000	460	0.36	14.6
InSb	10^{-7}	10^5	1700	0.18	17.7

4

$$\underbrace{\frac{\Delta n}{\tau}}_{\text{recombination}} - \underbrace{D_n \frac{\mathrm{d}^2}{\mathrm{d}z^2}\Delta n}_{\text{diffusion}} = \underbrace{\alpha \Phi_0 \mathrm{e}^{-\alpha z}}_{\text{source}} \qquad (11.7)$$

The solution to this equation is the sum of a particular solution including a source term and a general solution without a source term, i.e:

$$\Delta n(z) = A\mathrm{e}^{-z/L_D} + B\mathrm{e}^{z/L_D} + \frac{\alpha \tau \Phi_0}{1-(\alpha L_D)^2}\mathrm{e}^{-\alpha z} \qquad (11.8)$$

Surface recombination S (in $\mathrm{cm\,s^{-1}}$) at $z = z_0$ imposed as:

$$S\Delta n|_{z=z_0} = D\left(\frac{\mathrm{d}}{\mathrm{d}z}\Delta n\right)_{z=z_0} \quad (11.9)$$

Ohmic contact, i.e. an interface where the recombination of minority carriers is instantaneous (an ohmic p^+ contact on p-type material imposes a density of minority carriers n given by $np = n_i^2$, i.e. $n \approx 0$) such that:

$$\Delta n|_{z=z_0} = 0 \quad (11.10a)$$

Space charge region starting at $z = z_0$, i.e. a region out of which all carriers are swept, and again leading to:

$$\Delta n|_{z=z_0} = 0 \quad (11.10b)$$

6

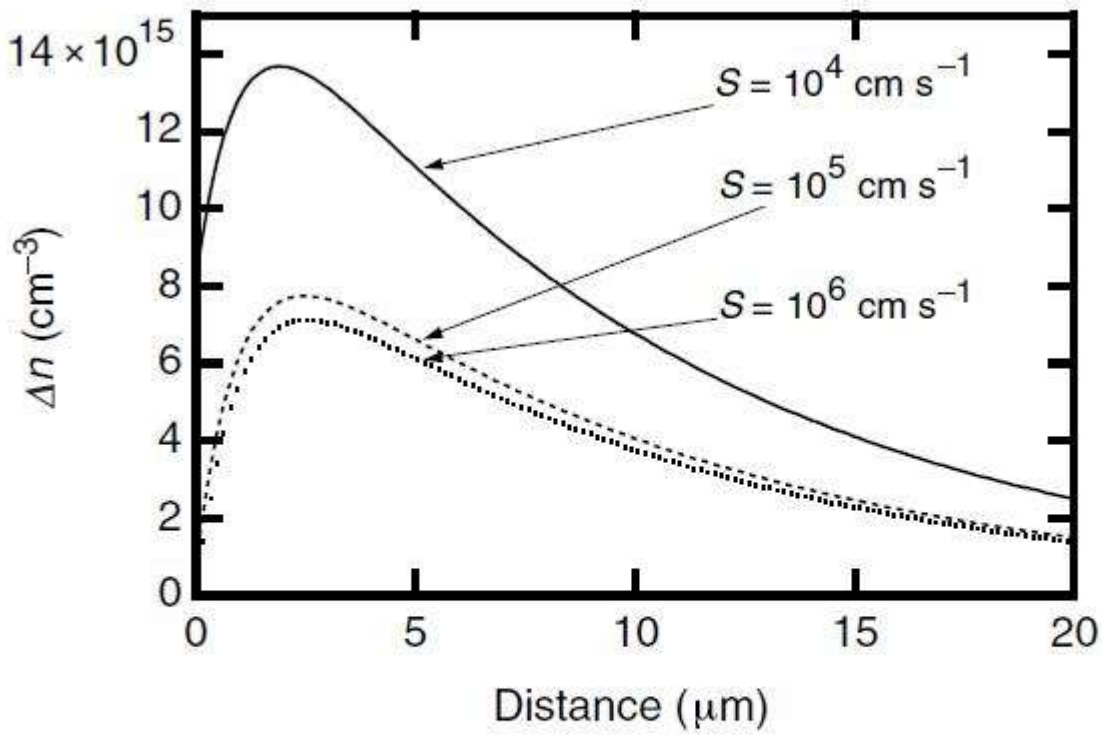

Fig. 11.3. Distribution of photogenerated carriers for a photon flux $\Phi_0 = 10^{18}\,\text{cm}^{-2}$, a diffusion coefficient of $1\,\text{cm}^2\,\text{s}^{-1}$, a diffusion length of 10 μm, and an absorption coefficient of $10^4\,\text{cm}^{-1}$, for various surface recombination velocities S.

internal quantum efficiency η_i of the detector

$$\eta_i = \frac{\Delta n_{\text{tot}}/\tau}{\Phi_0} = 1 - e^{-\alpha d} \qquad (11.14a)$$

optical efficiency $\boxed{\eta_{\text{op}} = 1 - R.}$

$$R = (n_{\text{sc}} - 1)^2/(n_{\text{sc}} + 1)^2.$$

$n_{\text{sc}} = 3.4$ leading to $R = 0.3$ and $\eta_{\text{op}} = 1 - R = 0.7$.

The total efficiency η is

$$\boxed{\eta = \eta_i \eta_{\text{op}} = (1 - R)(1 - e^{-\alpha d}) \qquad (11.14b)}$$

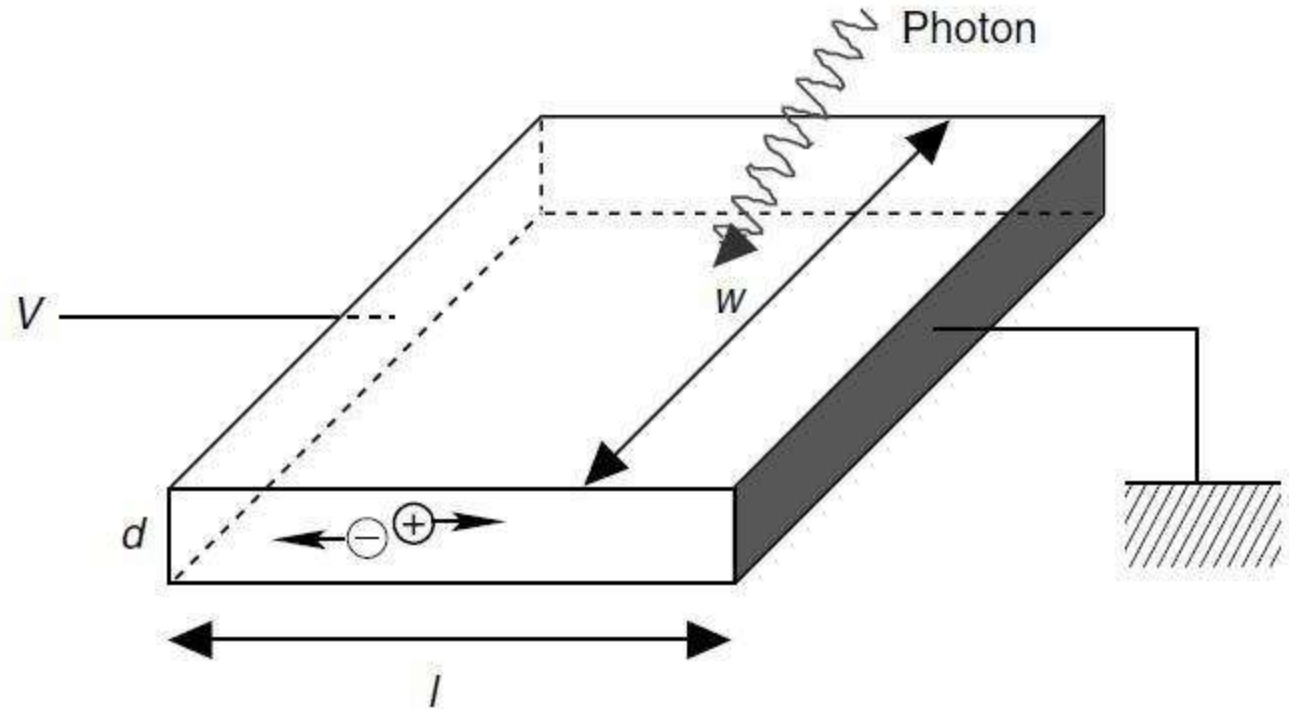

Fig. 11.5. Geometry for a photoconducting detector.

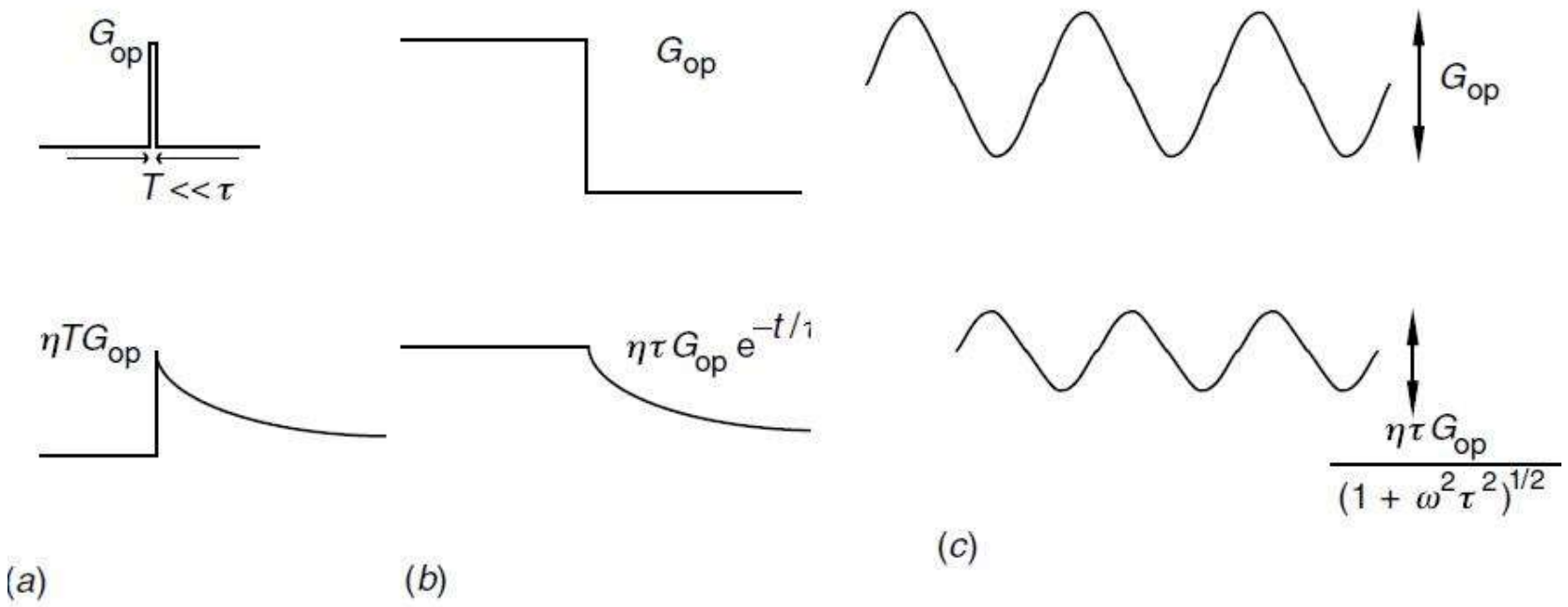

Fig. 11.7. Time response for a photoconductor subject to (*a*) abrupt pulse of illumination, (*b*) abrupt cessation of long pulse of illumination, and (*c*) sinusoidally varying illumination.

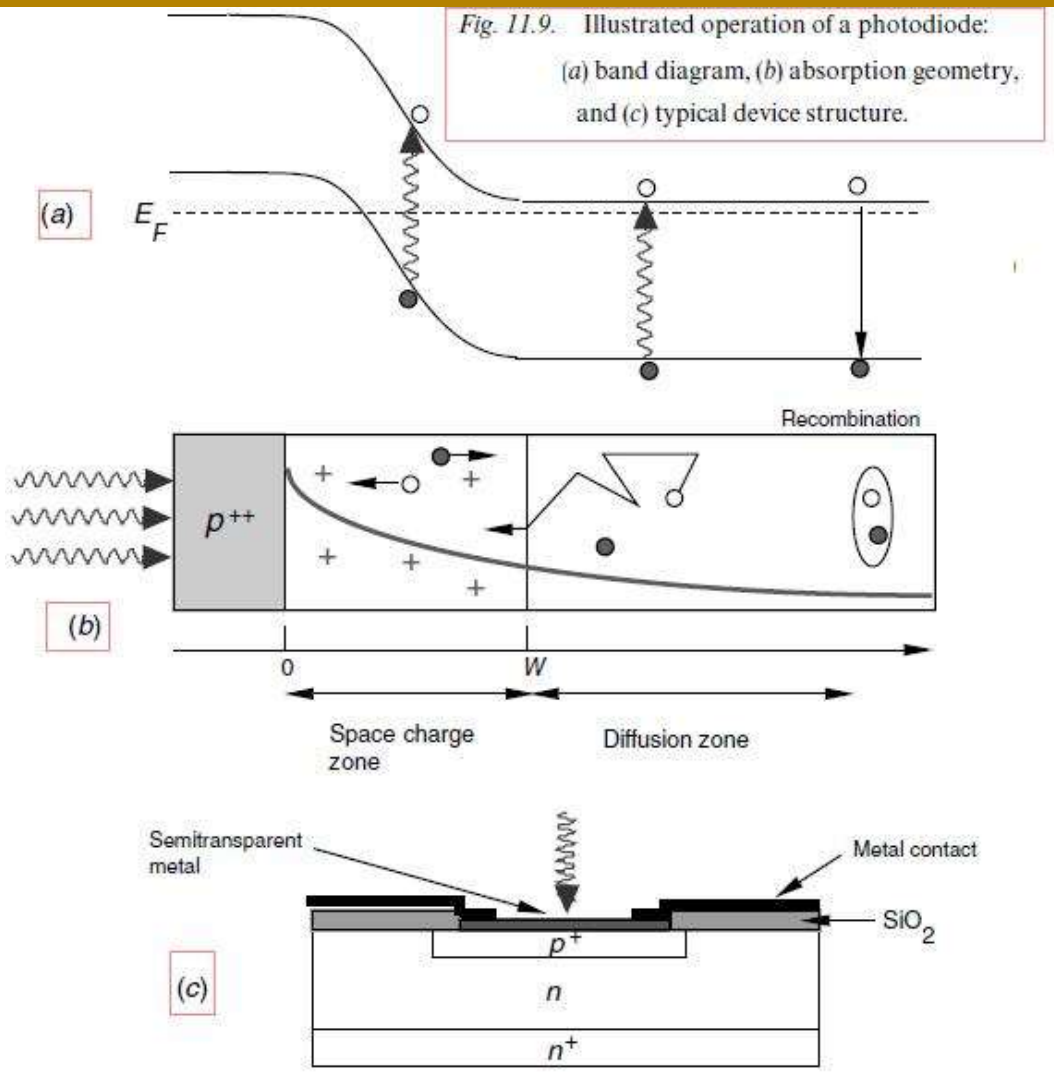

Fig. 11.9. Illustrated operation of a photodiode: (*a*) band diagram, (*b*) absorption geometry, and (*c*) typical device structure.

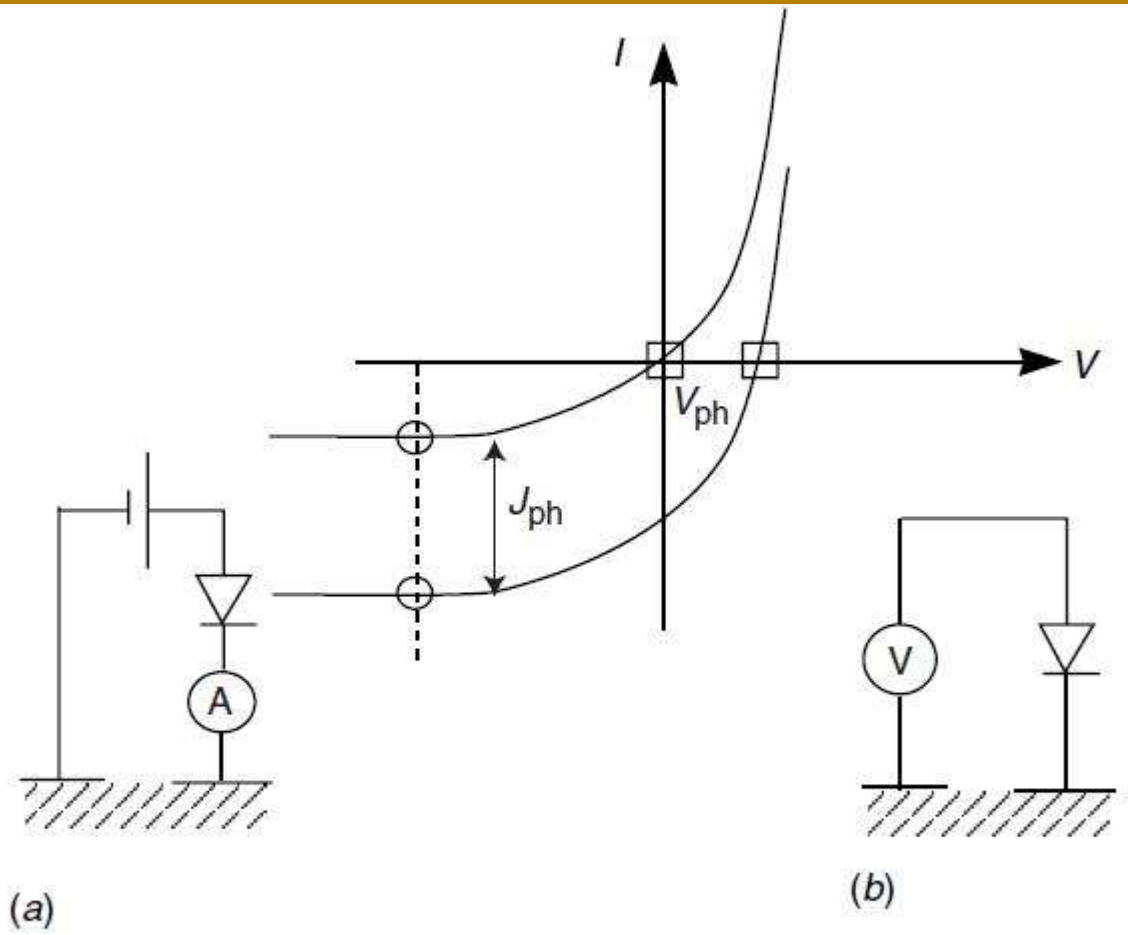

Fig. 11.10. Two operation modes for a photovoltaic detector: (*a*) photocurrent mode, and (*b*) photovoltage mode.

concentration can only be zero ($np^+ = n_i^2$), so that $J_G(0) = 0$ and:

$$J_G = -q\Phi_0(1 - e^{-\alpha W}) \tag{11.35}$$

This is the electron current that crosses the boundary between the SCR and the neutral material at $z > W$.

The contribution of the diffusion current is obtained from the differential equations (11.3a) or (11.7) which at stationary state admit as a solution expression (11.8), which we rewrite here as:

$$\Delta n(z) = Ae^{-z/L_n} + Be^{z/L_n} + \frac{\alpha\tau\Phi_0 e^{-\alpha W}}{1 - (\alpha L_D)^2} e^{-\alpha z} \tag{11.36}$$

given that the photon flux at $z = W$ is now only $\Phi_0 e^{-\alpha W}$. We may suppose that the sample is sufficiently thick to assume $B = 0$. Furthermore, every electron at $z = W$ is immediately swept by the electric field imposed by boundary condition (11.10b) $\Delta n(W) = 0$ such that:

$$\Delta n(z) = \frac{\alpha\tau\Phi_0 e^{-\alpha W}}{1 - (\alpha L_D)^2} (e^{-\alpha(z-W)} - e^{-(z-W)/L_n}) \tag{11.37}$$

The diffusion current density at $z = W$ is given by:

$$J_{\text{diff}} = +qD_n \frac{\mathrm{d}}{\mathrm{d}z}\Delta n|_{z=W} \tag{11.38}$$

that is

$$J_{\text{diff}} = -q\frac{\alpha L_D}{1+\alpha L_D}\Phi_0 \mathrm{e}^{-\alpha W} \tag{11.39}$$

For the relatively common condition where $\alpha W \approx 1$, the contributions made by J_G and J_{diff} ((11.35) and (11.39), respectively) are comparable so that neither of the two terms can be neglected. The total photocurrent is then given by:

$$J_{\text{ph}} = -q\Phi_0\left(1 - \frac{\mathrm{e}^{-\alpha W}}{1+\alpha L_D}\right) \tag{11.40}$$

This formula indicates that the low quantum efficiency of the space charge region $\mathrm{e}^{-\alpha W}$ can be regained once the diffusion length becomes large, i.e. what the space charge region lets through, is recuperated by the diffusion region. Expression (11.40) can, as in the photoconductor case, be put into the form:

$$\mathscr{R} = \eta\frac{1}{h\nu/q} \tag{11.41}$$

or alternatively as:

$$\mathscr{R} = \eta \frac{\lambda(\mu\text{m})}{1.24} \tag{11.42}$$

with a total *quantum efficiency* η given by:

$$\eta = (1 - R)\left(1 - \frac{e^{-\alpha W}}{1 + \alpha L_D}\right) \tag{11.43}$$

This formula is therefore quite similar to (11.18). We note, however, the absence of photoconductive gain, which is equivalent to saying that the gain g in a photodiode is unity.

Example

In *n*-type silicon doped $10^{16}\,\text{cm}^{-3}$, the SCR extends across 1 μm for a junction potential $V_{\text{bi}} = 1$ V. Figure 11.2 shows an absorption coefficient $\alpha = 10^4\,\text{cm}^{-1}$ at 2 eV. The efficiency of the SCR $1 - e^{-\alpha W}$ is then 64%. On the other hand, the diffusion length is $\sqrt{((kT/q)\mu_n\tau)}$ or 500 μm (see Table 11.1), which leads to a quantum efficiency dominated by the reflectivity $(1 - R)$.

11.4.1 Photodiode detectivity

As discussed in Complements 11.A and 11.B, two mechanisms are responsible for noise in photovoltaic detectors: generation noise (without recombination) i_G (11.A.38) and photon arrival fluctuation noise (11.B.6). Again, we will make the assumption that the detector noise is not dominated by photon noise (i.e. that the detector is not in the BLIP regime – see Complement 11.B). The noise due to the detector itself is then:

$$i_N^2 = 2qI_0\Delta\nu = 2qI_{sat}(1 + e^{qV/kT})\Delta\nu \tag{11.44}$$

where I_{sat} is the saturation current of the photodiode. The general idea behind (11.44) is that the 'plus' sign in (11.44) results from the fact that the forward and reverse contributions cancel out at $V = 0$, while their respective contributions to the noise are additive. The signal-to-noise ratio (S/N) is given by:

$$\frac{i_S}{i_N} = \frac{\mathscr{R}P_{inc}}{\sqrt{2qI_{sat}(1 + e^{qV/kT})\Delta\nu}} \tag{11.45}$$

and the *noise equivalent power* (NEP) takes the form of:

$$\text{NEP} = \frac{\sqrt{2qI_{sat}(1 + e^{qV/kT})\Delta\nu}}{\mathscr{R}} \tag{11.46}$$

The signal-to-noise ratio (S/N) is given by:

$$\frac{i_S}{i_N} = \frac{\mathscr{R} P_{\text{inc}}}{\sqrt{2qI_{\text{sat}}(1 + e^{qV/kT})\Delta v}} \tag{11.45}$$

and the *noise equivalent power* (NEP) takes the form of:

$$\text{NEP} = \frac{\sqrt{2qI_{\text{sat}}(1 + e^{qV/kT})\Delta v}}{\mathscr{R}} \tag{11.46}$$

We reintroduce the *detectivity* D^* as it allows us to get rid of parameters that are not intrinsic to the system: (i) the area A, which relates the current I_{sat} to the

current density J_{sat} ($I_{sat} = AJ_{sat}$), and the flux Φ_0 to the incident power P_{inc} ($P_{inc} = A\Phi_0 h\nu$); and (ii) the frequency measurement bandwidth $\Delta\nu$:

$$D^* = \frac{\mathscr{R}}{\sqrt{2qJ_{sat}(1 + e^{qV/kT})}} \tag{11.47a}$$

We insist again on the fact that this time, the detection area and the transport area are one and the same. The photon and electron fluxes are parallel.

We may think it profitable to bias the diode ($V < 0$) to decrease the factor $e^{qV/kT}$ and increase the photodiode detectivity. This bias, however, often adds additional noise (peripheral leakage current, . . .) to the detection signal. Under zero applied bias ($V = 0$), (11.47a) becomes:

$$D^* = \frac{\eta}{h\nu/q} \frac{1}{\sqrt{4qJ_{sat}}} \tag{11.47b}$$

This expression can be written in another form, by noting that:

$$\left.\frac{dj}{dV}\right|_{V=0} = \frac{1}{RA} = \frac{q}{kT} J_{sat} \tag{11.48}$$

where RA ($\Omega\,cm^2$) is the product of the junction resistance with its area such that:

$$D^* = \frac{\eta}{h\nu/q}\sqrt{\frac{RA}{4kT}} \tag{11.49}$$

Photodiode detectivity

Figure 11.11 shows how detectivity D^* varies as a function of the product RA at different temperatures for a detection wavelength of 5 μm ($h\nu = 250$ meV) and a quantum efficiency of 50%.

This last formula is quite predictive when coupled with the expression for the current density j_{sat} in a junction (10.B.4), i.e:

$$j_{sat} = \frac{qD_p}{L_{Dp}}\frac{n_i^2}{N_D} = q\sqrt{\frac{D_p}{\tau_p}}\frac{n_i^2}{N_D} = q\sqrt{\frac{D_p}{\tau_p}}\frac{N_c N_v}{N_D}e^{-E_g/kT} \tag{11.50}$$

where we recall that D_p, L_{Dp}, and τ_p are the diffusivity, diffusion length, and lifetime of the minority carriers (holes) on the n side of the junction; N_D is the doping concentration; n_i is the intrinsic carrier density given in (5.49); E_g is the detector bandgap; and N_c and N_v are the effective state densities in the conduction and valence bands given in (5.46). Therefore the detectivity outside of the detector's BLIP regime varies as $e^{-E_g/2kT}$, which emphasizes the interest in operating these detectors at low temperature. We can also use (10.B.3) if the diode leakage current is dominated by generation–recombination occurring at impurity sites.

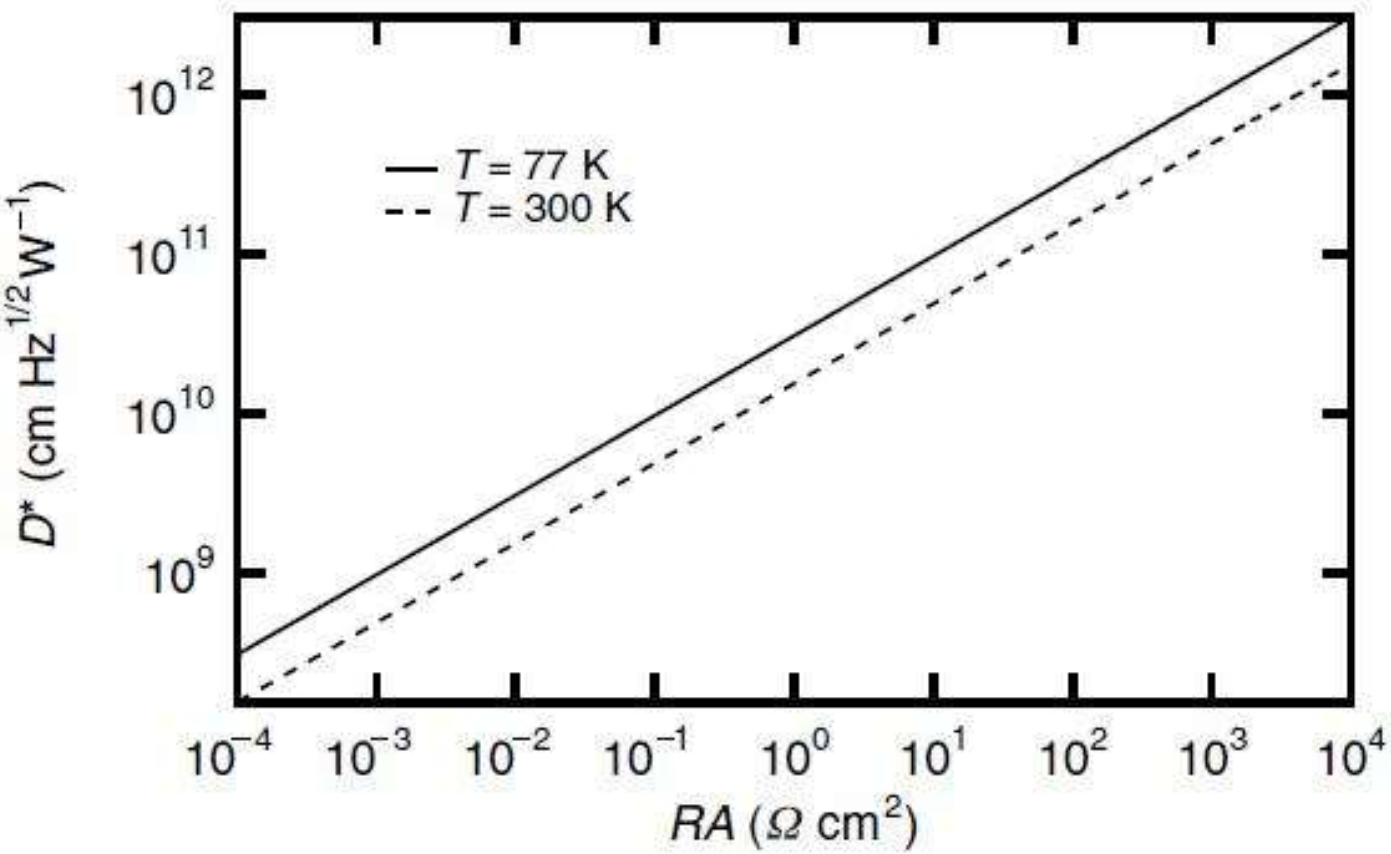

Fig. 11.11. Variation in photodiode detectivity at 5 μm as a function of RA (a quantum efficiency of 50% is assumed).

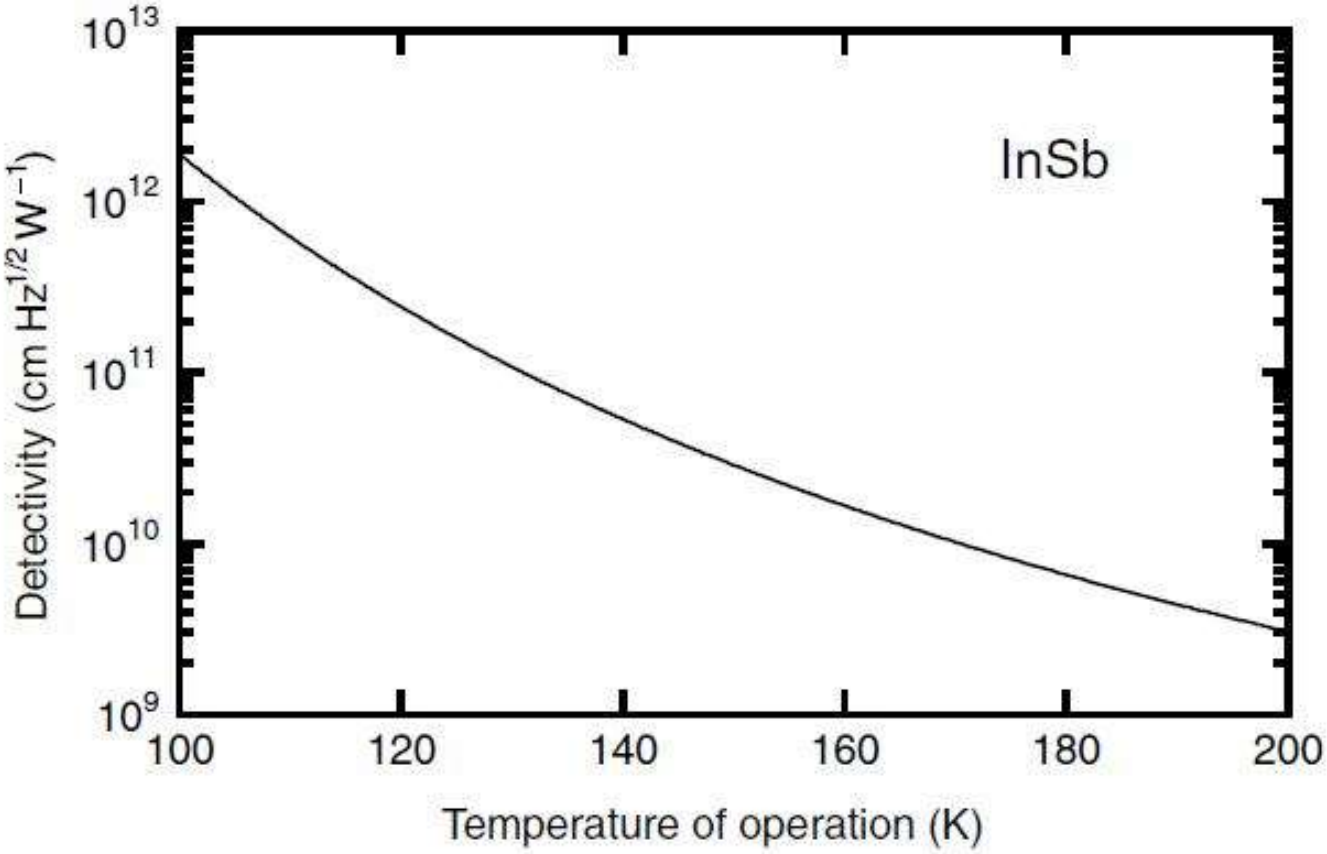

Fig. 11.12. Detectivity as a function of temperature for a *p–n* InSb photodiode.

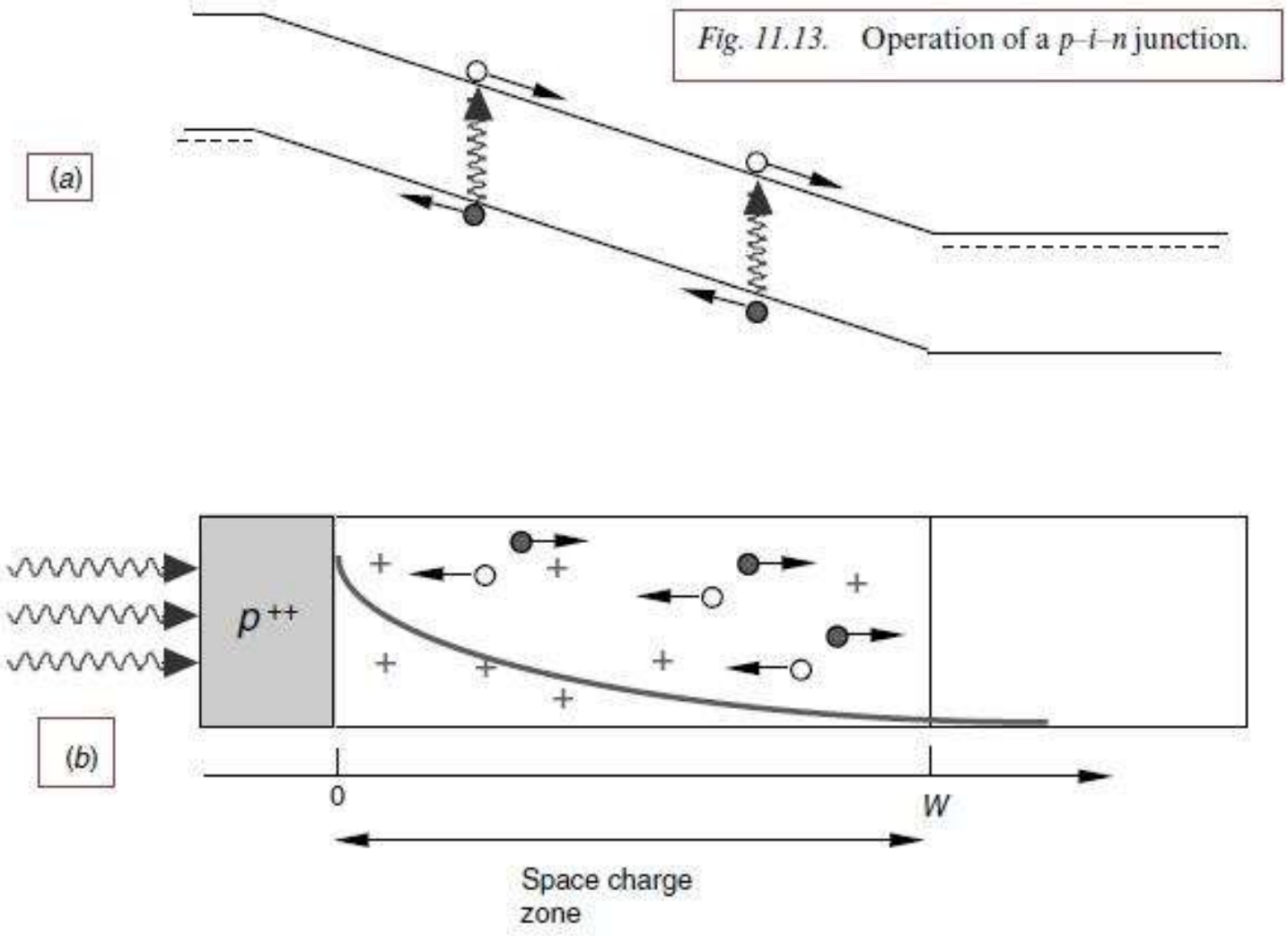

Fig. 11.13. Operation of a *p–i–n* junction.

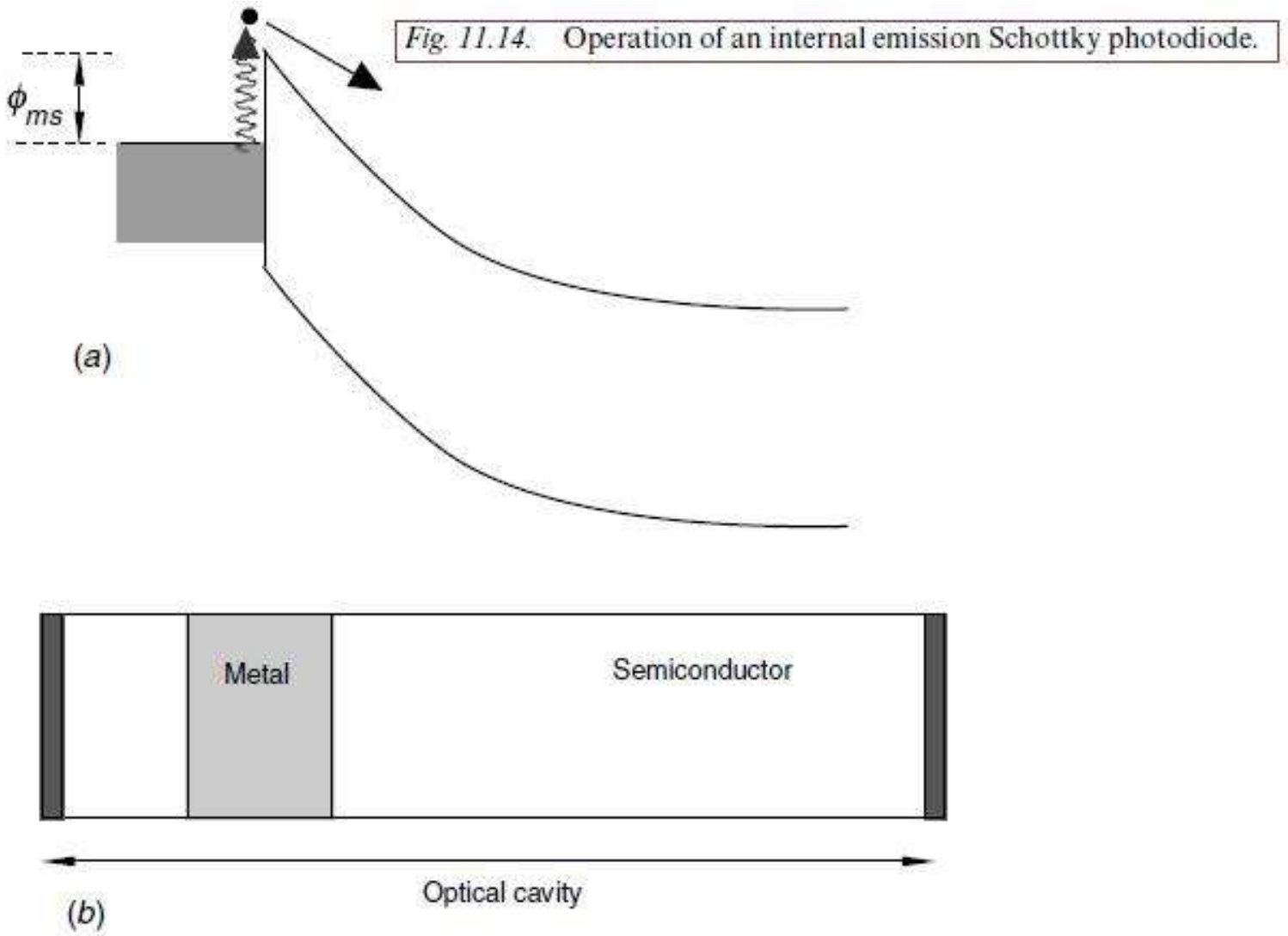

Fig. 11.14. Operation of an internal emission Schottky photodiode.

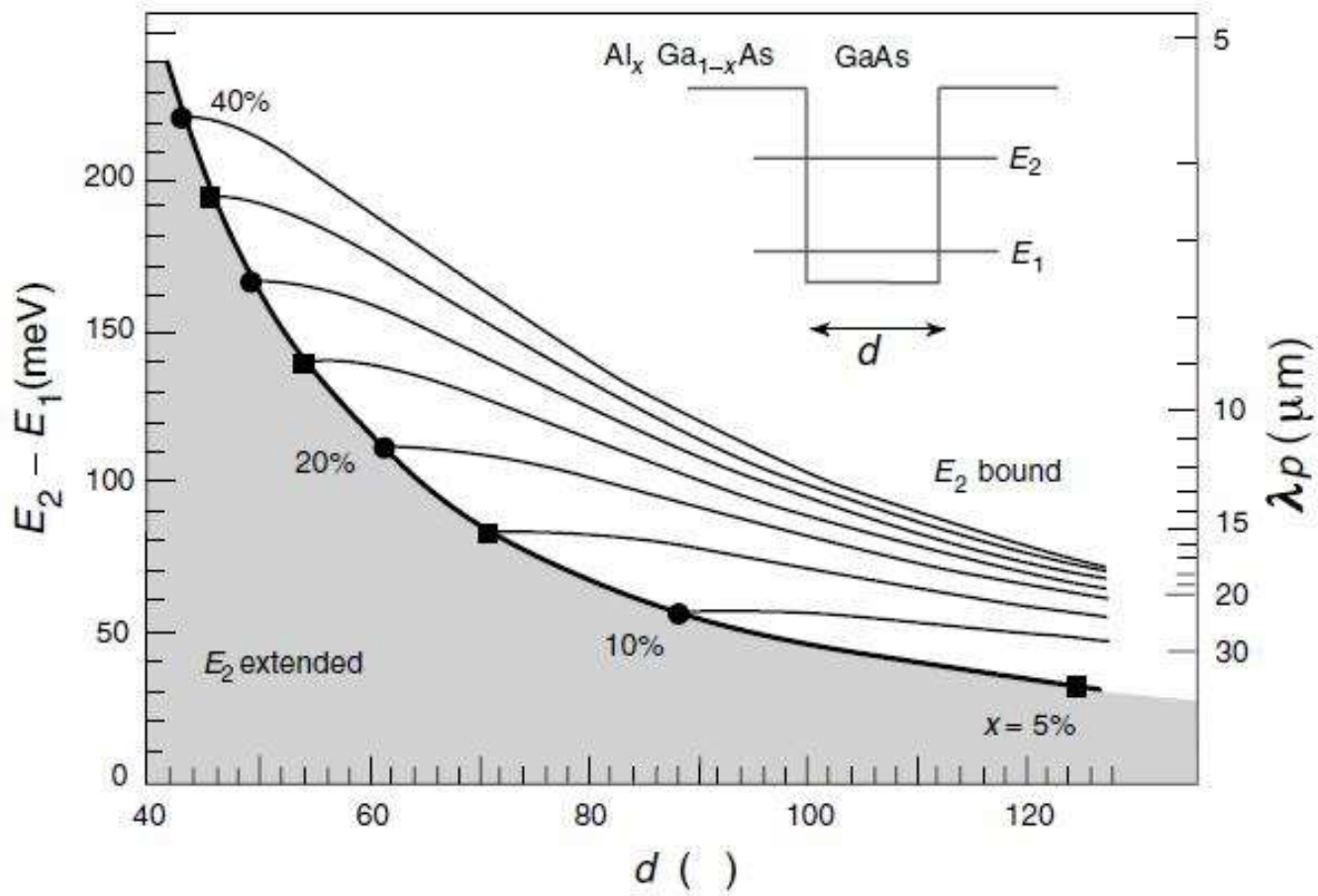

Fig. 11.17. Energies for bound-to-bound (narrow curves), bound-to-free (shaded region), and bound-to-quasi-resonant (thick curve) transitions in GaAs/$Al_xGa_{1-x}As$ quantum wells.

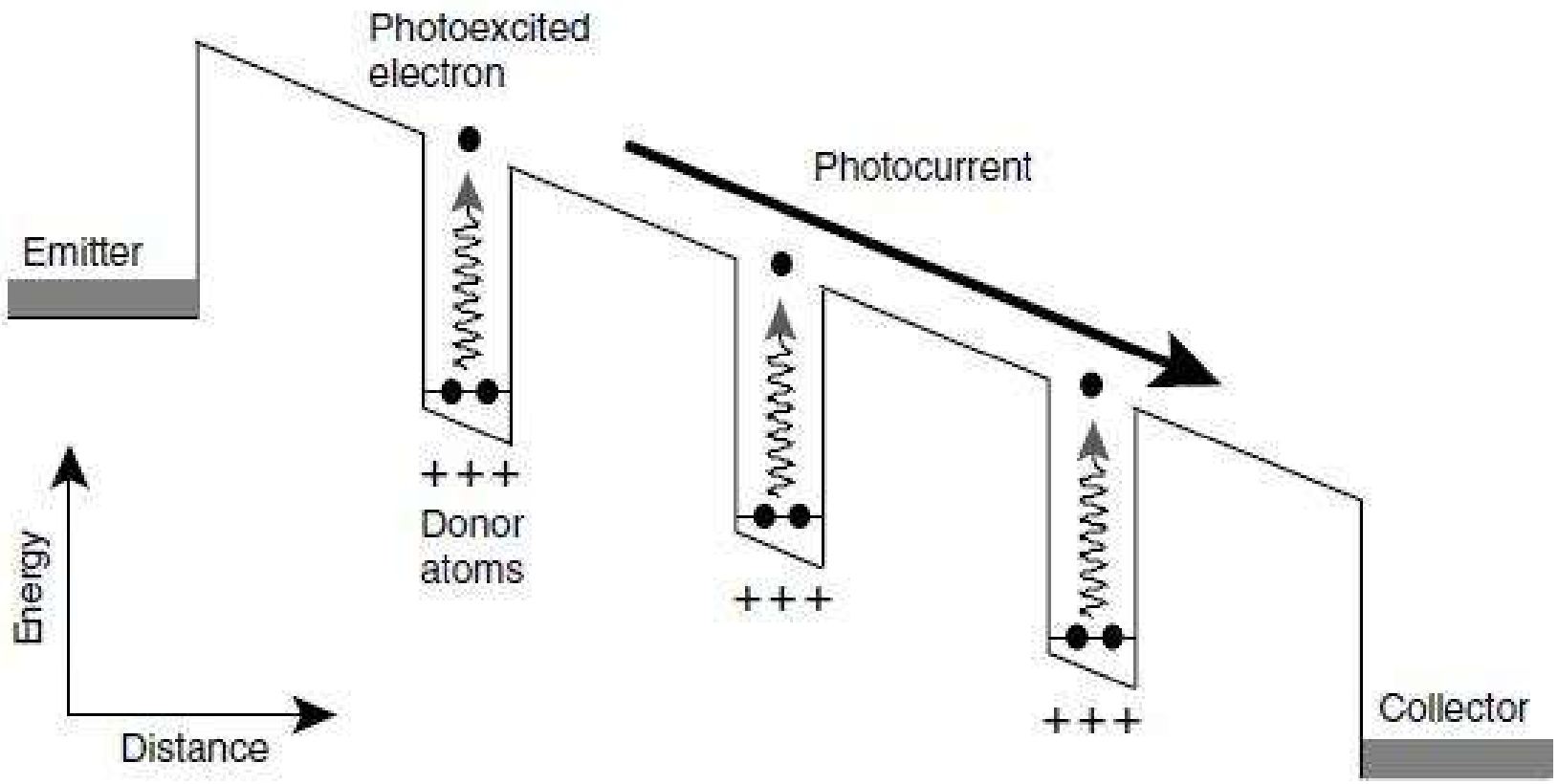

Fig. 11.18. Operation of a multiple quantum well detector.

25

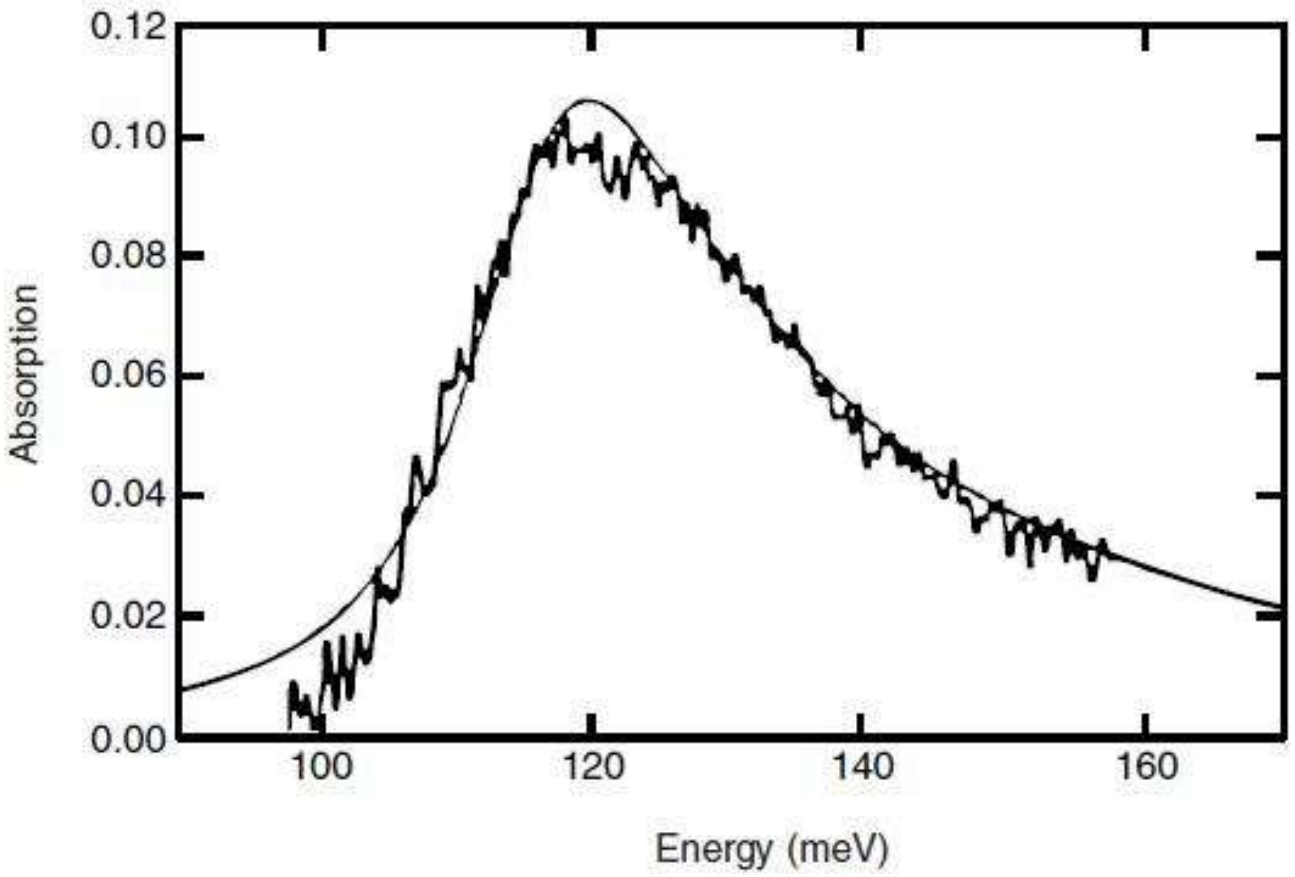

Fig. 11.19. Experimental and calculated absorption spectra for a multi-quantum well detector in a planar waveguide geometry ($\theta = 90°$). (Courtesy of F. Luc@THALES.)

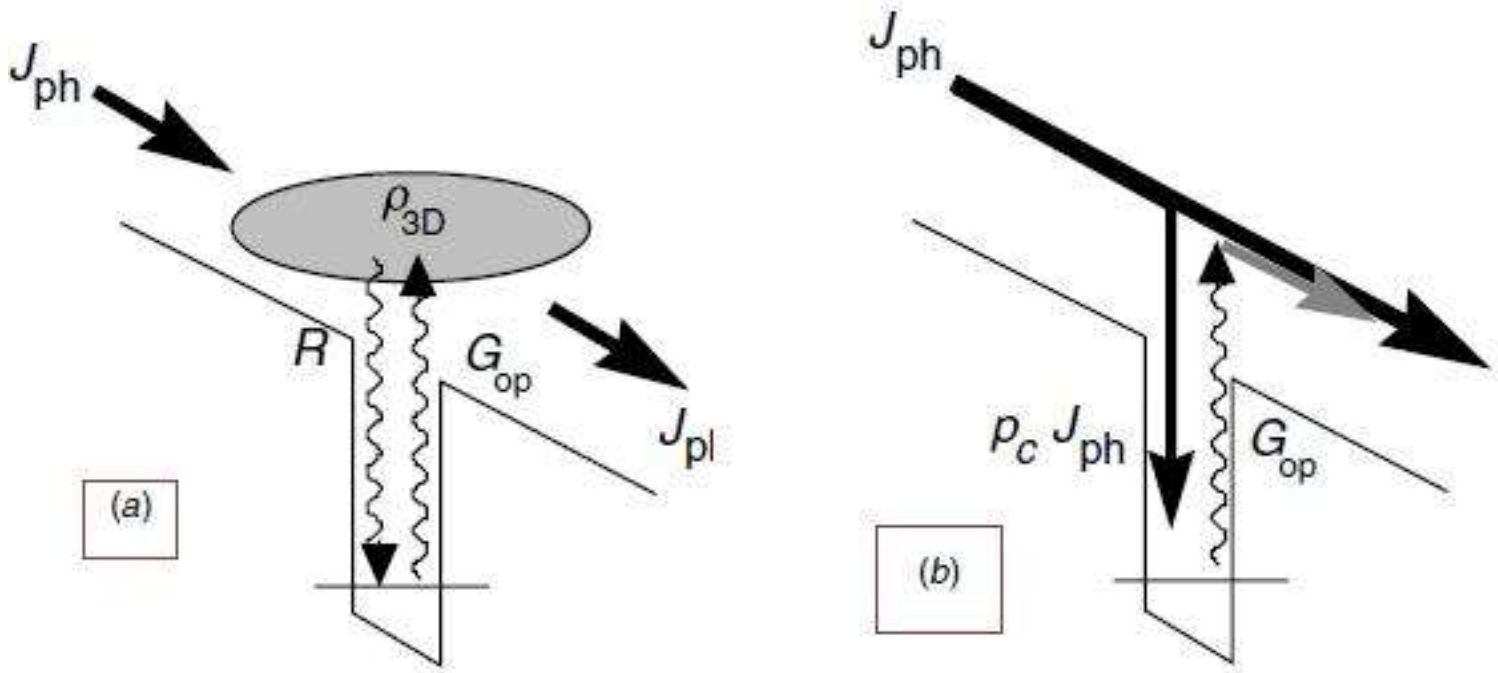

Fig. 11.20. Two models for electron transport across a multiple quantum well detector: (*a*) photoconduction model and (*b*) photoemission model.

27

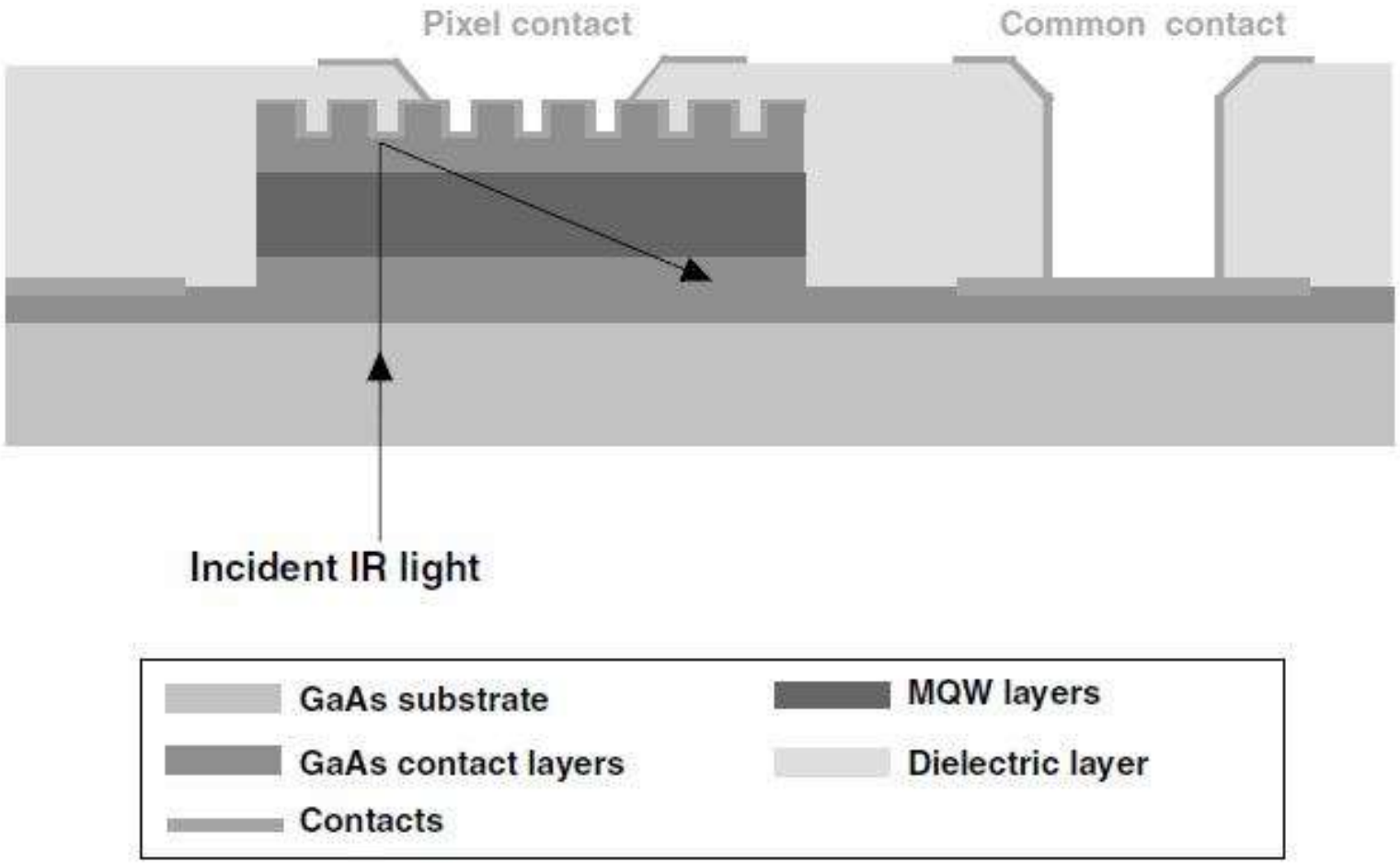

Fig. 11.22. Single pixel in a multiple quantum well detector array. A grating coupler redirects normally incident light to increase overlap with allowed intersubband transitions.


Clip۲ni.com